Effect of Pressure Gradient on the Evaporation Rate from a Horizontal Water Panel

تأثير التدرج فى الضغط على معدل التبخر من حوض مائى أفقى

G. I. Sultan
Mechanical Power Engineering Department,
Faculty of Engineering, Mansoura University, Mansoura, Egypt.
Email:gisultan@mans.edu.eg

الخلاصة:

تم عمل دراسة تجريبية لإنتقال الكتلة لسريان منتظم لهواء يمر على سطح الماء الموجود فى حوض مستطيل مثبت فى قاعدة نفق هوائى ذو تدرج فى الضغط. ولإحداث تدرج فى الضغط يتم تغيير المقطع المار خلاله الهواء عن طريق وضع أجنحة مستوية بزوايا ميل مختلفة على جانبى النفق الهوائى. وقد تم حساب رقم شروود عند قيم مختلفة لرقم رينولدز (51670>Re>11000) و زوايا ميل مختلفة (7.8° >θ>0.0). وقد أظهرت النتائج أن رقم شروود يزيد مع زيادة رقم رينولدز مع وجود تدرج موجب أو سالب فى الضغط. وأيضا رقم شروود يزيد مع زيادة التدرج فى الضغط فى المقطع المجمع وتصل هذه الزيادة إلى 297% عند رقم رينولدز Re=11000 . وقد تم إستنتاج صيغة رياضية لابعدية لحساب رقم شروود كدالة فى رقم رينولدز ورقم شميت وكذلك التدرج فى الضغط .

ABSTRACT:

The rate of evaporation from a water panel to air flow in a wind tunnel is investigated experimentally. A turbulent air is flowed in a rectangular duct (11000<Re<51670). Wedges are fixed on the inner vertical walls of the test section above the water panel. The influence of area ratio parameter (β) on the evaporation rate and hence the mass transfer coefficient is considered at different values of Reynolds number. The results show that, Sherwood number increases with increasing Reynolds number for both negative and positive pressure gradient. Also, Sherwood number increases with increasing the area ratio parameter, which is proportional to the pressure gradient for all values of Reynolds number in case of convergent configuration. But it decreases with the increase in positive pressure gradient in case of divergent configuration. The maximum enhancement in mass transfer coefficient in case of negative pressure gradient is 297% at Re=11000 and β=0.06898. An empirical correlation for Sherwood number as a function of Reynolds number, Schmidt number and area ratio parameter for the considered operating conditions are obtained.

Key words: Evaporation, mass transfer, duct flow.

INTRODUCTION:

The evaporation of liquid into a gas flow is of great importance in many chemical and mechanical engineering processes. Evaporation of water into an air stream has received a considerable attention due to its widespread applications, such as in drying, air conditioning ...etc. Flow with adverse pressure gradient which occurs in many engineering applications, is often characterized by flow separation. It produces an adverse influence on the performance of such applications. Thus, it has a considerable interest to be studied for flow in ducts, which containing separated regions. Araid (1975), has found experimentally that the coefficient of heat transfer by convection from a flat plat surface to air depends on the velocity distribution around the surface and proposed a correction factor for the Nusselt equation when calculating the coefficient of heat transfer. He also found that this factor has a value between 0.52 and 1.7 in his experiments according to the type of the stream flow. Hesse et al., (1976), studied experimentally the film boiling of Carbon dioxide covering a pressure range from the triple

Accepted March 31, 2002

point to critical point. Berger and Hau (1979), used an electrochemical analogy technique to determine the heat transfer distribution in pipes roughened with square small ribs. A three dimensional model had been given by Palaszewski et al., (1981). They computed the local variation in the dry bulb temperature, absolute humidity and streamlines throughout the flow field and their effect on local variation of drop cooling. A numerical investigation to study the evaporation rate of water into laminar stream of air, humid air and superheated steam over a flat plate was performed by Chow et al. (1983). They used equations of heat and mass transfer, and derived an iterative similarity solution to the problem. Their results show that, below the inversion temperature of the free stream, water evaporation decreases as the humidity of air increases; and above the inversion temperature, water evaporation increases as the humidity of air increases. Awad et al., (1986) studied experimentally the heat transfer through a periodically converging-diverging duct to airflow. Their results showed 50% increase in the heat transfer coefficient and the pumping power is increased by 23.8%. Han et al., (1991), investigated the effect of the agitated rib angle orientation on local heat transfer distributions and on the pressure drop in a square channel with two opposite in-line ribbed wall. The effects of steam content on the rate of evaporation of water into humid air and superheated steam at elevated temperatures is studied experimentally by Sheikholeslami et al.(1992). Their results show that, the evaporation rates during the heat transfer controlled period are higher in superheated steam than in relatively dry air at inversion temperature greater than 180°C. While the relationship is reversed at inversion temperature lower than 180°C. Zheng and Worek (1996), investigated the distribution of local heat and mass transfer coefficients in an evaporation process at the air liquid interface and to determine the effect of introducing rods to disturb the liquid and air flow field, and to enhance the heat and mass transfer rates. Kachhwaha et al., (1998), developed a two-dimensional model simulating the conservation of mass, momentum and energy of water spray drops and air stream in a parallel flow configuration. Also, their experimental results indicated that dry bulb temperature decreased 9°C by employing evaporative cooling during dry summer months. Kachhwaha et al.(1998), developed a simple and efficient numerical model for estimation of heat and mass transfer between water spray drops and air stream in a horizontal counter flow configuration to enable accurate prediction of evaporative cooling performance. Sultan et al.,(1999), investigated experimentally the effect of inlet parameters for air and desiccant on the output variables. They found that the evaporation rate of water from desiccant increased with increasing air and solution inlet flow rates and temperatures. Also, the regeneration rate decreased with increasing humidity ratio of inlet air and solution inlet concentrations. Cox and Yao, (1999), performed experimentally the heat transfer of mono-disperse sprays of large droplet diameters on high temperature surface. A theoretical study of the evaporation of water into air and superheated steam is performed by Schwartze et al. (2000). Their model is a useful tool for the prediction of evaporation rates and the inversion temperature. Also, it helps in the design of drying processes and estimation of the feasibility of different process options. Rabie et al., (2001) presented an experimental study for flow and heat transfer in turbulent airflow in a periodically varying cross-sectional area annular tube. Their results showed that friction losses as well as heat transfer of variable cross-sectional annulus are higher than that of constant cross-sectional area.

In the present work, the influence of the area ratio parameter of the wedges on mass transfer from water panel to air flow inside the duct (Sherwood number) is investigated experimentally at different values of Reynolds number.

EXPERIMENTAL TEST RIG:

The schematic diagrams of the experimental apparatus and the test section are shown in figure(1) and figure(2). The test rig is consisted mainly of a rectangular wind tunnel with

different cross sectional area to achieve the required pressure gradient for the forced air which flows over the surface of the water panel (13). Air is withdrawn from the ambient by an air blower (12), which is connected to the rectangular wind tunnel (3) using a flexible connection (9) to absorb the vibration from the fan. A certain cone is connected to the end of the test section followed by a circular tube and then a calibrated orifice meter (6) installed and is connected to a micro-manometer (8) of a scale division 1 Pa to measure the air flow rate through the wind tunnel. A plate gate valve (7) at the outlet of the wind tunnel is used to change the air flow rate through the test section. A screen and bell-mouth inlet (1&2) is introduced at the wind tunnel inlet to ensure uniform velocity distribution at inlet of the test section (11). The dry Bulb and wet bulb temperatures at upstream and downstream of the water panel are measured by four thermometers (4 and 5) with scale division of 0.5 °C. Air is passed through the test section of 1800 mm long with 160 mm x 156 mm cross sectional area. A water panel (13) of 400 mm long, 160 mm wide, and 30 mm depth is located at 1200 mm from the test rig inlet.

A pair of wooden wedges (14) is used to create pressure gradient over the surface of water panel along the airflow. The wooden wedges are fixed on the inner vertical walls of the rectangular cross section of the test rig above the water panel using rubber silicon as shown in Fig.(2). Five pairs of wooden wedges "for both convergent and divergent configurations" are used, whose dimensions are given in Table (1). The mass of water in the panel is measured before and after each experiment by using a digital mass balance (10) with a scale division of 0.1 g. The static pressure at inlet and exit of the test section is measured by a micro-manometer through the pressure taps (15) with a scale division of 1 Pa.

Table (1) Dimensions of wooden wedges

δ, m	δ/L	θ, deg.	$\Delta A=A_e-A_i$ m^2	A_{av}, m^2	$\Delta A/A_{av}$	$\beta = \delta/L\,(\Delta A/A_{av})$
0.00 "Zero pressure gradient"	0.00	0.000	0.00	0.01497	0.00	0.00
0.02	0.05	2.862	0.00384	0.01306	0.2941	0.01471
0.03	0.075	4.289	0.00576	0.01209	0.4761	0.03571
0.04	0.10	5.711	0.00768	0.01113	0.6898	0.06898
0.05	0.125	7.125	0.00961	0.01017	0.9434	0.11792
0.055	0.1375	7.829	0.01055	0.00969	1.0887	0.14969

Where:

- A_e exit area of the test section
- A_i inlet area of the test section
- ΔA change in area, $\Delta A = A_e - A_i$
- A_{av} average area, $A_{av}=(A_e+A_i)/2$
- L wedge length
- β area ratio parameter, $\beta = \delta/L(\Delta A/A)$
- δ wedge thickness
- θ wedge angle

DATA REDUCTION:

For each experimental test, measurements of all variables " DBT_I, WBT_I, m_w, T_W, time, and pressure at inlet and exit of the test section" were recorded after steady state was establishment. The effect area ratio parameter on the evaporation rate and mass transfer coefficient were studied and compared with the previous results.

The air-water vapor mixture is dilute and thus I use dry air properties for the mixture at a bulk temperature $T_B = (T_o + T_w)/2$.

Where T_B, To and T_w are the bulk temperature and free stream temperature and water temperature in the panel, respectively.

Reynolds number was calculated from:

$$\mathrm{Re} = \frac{u_\infty D_H}{\nu} \qquad (1)$$

Where:

u_∞ free stream velocity.
ν kinematic viscosity calculated at air bulk temperature.
D_H characteristic length,

$$D_H = \frac{4\,Volume\,occupied\,by\,the\,flow}{Wetted\,surface\,area} = \frac{4\left[(W-\delta)L\right]H}{2\left[(W-\delta)L + H\sqrt{L^2+\delta^2}\right]} \qquad (2)$$

W width of the test section

The vapor density in humid air just above the surface of the water in the panel is calculated from the following relation [10]:

$$\rho_w = M_{H_2O}\frac{\rho_a}{M_a}X_w \qquad (3)$$

Where:

ρ_a dry air density
ρ_w water vapor density
M_{H2O} molecular weight of water vapor
M_a molecular weight of air
X_w mole fraction of water vapor at the interface, $X_w = P_{sat}/P_{atm}$,
P_{atm} atmospheric pressure
and P_{sat} saturation pressure of water vapor in air at a temperature equal to the dbt.

The dry air mole fraction is calculated as follows:

$$X_\infty = \frac{P_v}{P_{atm}} \qquad (4)$$

$$P_v = \phi P_{sat} \qquad (5)$$

Where:

P_v partial pressure of water vapor at the interface.
ϕ relative humidity

The diffusion coefficient of water vapor is given by the relation [9]:

$$D = 1.87.10^{-10}\frac{T_w^{2.072}}{P_{atm}} \qquad (6)$$

Where:

D diffusion coefficient of water in air
P_{atm} atmospheric pressure

So, the Sherwood number and the mass transfer coefficient are calculated from the following relations:

$$Sh = \frac{h_m D_H}{D} \tag{7}$$

$$h_m = \frac{\dot{m}_w}{A(\rho_w - \rho_\infty)} \tag{8}$$

Where:

A	surface area of water panel, A= (W - δ) L
h_m	mass transfer coefficient
$\dot{m}_w$	evaporation rate
ρ_∞	vapor density in the free stream air.

RESULTS AND DISCUSSIONS:

The object of the experimental measurements is to determine the rate of evaporation (mass transfer coefficient and consequently Sherwood number) at different values of Reynolds number for the air flow inside a rectangular duct with existing pressure gradient.

In order to examine the reliability of the test rig, the present experimental results of Sherwood number versus Reynolds number in case of zero pressure gradient for air flow over a water panel, is compared with the corresponding published data as shown in Fig.(3). It is noticed that the present experimental results of the Sherwood number, as expected, increases with the increase of the Reynolds number and has a good agreement with results of [10].

In Fig. 4 the static pressure distribution along the panel length for convergent, (β<0.0) and divergent configurations (β>0.0) at absolute value of area ratio parameter β=0.14969 & Re=51670 are presented and compared with that of zero pressure gradient (β=0.0). As expected the static pressure decreases along the air flow in case of zero pressure gradient and convergent configuration, while it increases with direction of flow in case of divergent configuration.

Figure 5 shows the pressure gradient along the length of the water panel versus the area ratio parameter at different Reynolds number in case of convergent (β<0.0) and divergent (β>0.0) configurations. It is clear that the pressure gradient increases with increasing Reynolds number for all area ratio parameters.

Figure 6 indicates the variation of evaporation rate with area ratio parameter at different Reynolds number for convergent configuration. It is seen that the evaporation rate increases with increasing area ratio parameter until it reaches a certain values at which it begins to decrease. This is due to two distinct mechanisms. First, the negative pressure gradient associated with the flow through the convergent configuration extract the water vapor out of the pan and leads to the increase of evaporation rate. Secondly, the decrease in panel water temperature due to evaporation tends to decrease the diffusion coefficient. The maximum evaporation rate in case of negative pressure gradient is found to be 0.00045 kg/m^{2}s which corresponding to Re=51660 and β=-0.08.

Figure 7 indicates the variation of evaporation rate with area ratio parameter at different Reynolds number for divergent configuration. It is seen that the evaporation rate increases with increasing area ratio parameter until it reaches a certain values at which it begins to decrease. This is because the vapor pressure just above the interface is still less than that of without pressure gradient "as shown in Fig. 4" and this led to increase the evaporation rate. But at

certain value of area ratio parameter, the evaporation rate began to decrease because of the separation associated with the higher values of area ratio parameters. The maximum evaporation rate in case of divergent configuration is found to be 0.00027 kg/m^{2}s which corresponding to Re=51660 and β=0.069. The evaporation rate in case of convergent configuration is higher than the corresponding values in case of divergent configuration. This is because the positive pressure gradient associated with flow through divergent configuration leads to compress the diffusion boundary layer and this leads to a decrease of evaporation from the pan. While the negative pressure gradient associated with the flow through the convergent configuration extract the water vapor out of the pan and leads to the increase of evaporation rate. Also, the evaporation rate increases with increasing Reynolds number for the same area ratio parameter in case of convergent and divergent configurations.

Figures 8-9 show the dependence of the Sherwood number on the Reynolds number at different values of area ratio parameter β =0.01471, 0.03571, 0.06898, 0.11792 and 0.14969 in case of convergent and divergent configurations, and compared with that of zero pressure gradient. In all cases, it is seen that the Sherwood number in the case of convergent configurations is higher than that of divergent configurations and further greater than that of zero pressure gradient.

Figures 10-11 show the dependence of mass transfer coefficient ratio Sh/Sh_w on the Reynolds number at different values of area ratio parameters for both convergent and divergent configurations. The maximum enhancement in the Sherwood number is found to be about three times the corresponding value of no pressure gradient [Sh/Sh_w=2.97 at β=0.06898 and Re=11000] in the convergent configuration. The maximum enhancement in the Sherwood number is about twice the corresponding value of no pressure gradient [Sh/Sh_w=2.135 at β=0.06898 and Re=11000] in the divergent configuration. The enhancement ratio in mass transfer coefficients at different values of both Reynolds number and area ratio parameters are shown in table (2) for both convergent and divergent configurations

The present experimental data are used to obtain the dependence of average Sherwood number on the Reynolds number and area ratio parameter for both convergent and divergent configurations. The obtained results were correlated by statistical analysis to estimate the mass transfer parameter "Sherwood number" as a function of Reynolds number and area ratio parameter as shown in Fig.(12).

The regression equation obtained for both convergent and divergent configurations is:

$$Sh=(0.03698-0.08236\,\beta+0.33674\,\beta^2)\,\mathrm{Re}^{0.8}\,Sc^{1/3} \qquad (9)$$

Where:

$11000 \le \mathrm{Re} \le 51670$

$0.0 \le \beta \le 0.15$

The maximum deviation of the experimental data from this correlation is found to be ± 20%.

CONCLUSIONS:

An experimental investigation was conducted to study the effect of pressure gradient on the mass transfer coefficient for turbulent flow of air at different values of Reynolds number in a rectangular duct over a water panel. Evaporation of water to the air was determined by measuring the mass of water in the panel before and after each experiment.

The results show that:

1. Convergent pressure gradient leads to an increase in the mass transfer coefficient in all cases, and the maximum increase is found to be 297% at Re=11000 and β=0.06898.
2. The maximum enhancement in mass transfer coefficient in case of divergent pressure gradient is 213.5% at Re=11000 and β=0.06898, but in case of β=0.11792& β=0.1496 the mass transfer coefficients are less the corresponding values of no pressure gradient .
3. For the studied range of the operating parameters, an empirical correlation of the Sherwood number as a function of the Reynolds number and the area ratio parameter was obtained for turbulent air flow.

NOMENCLATURE:

A	surface area of the panel, m^2
D	diffusion of water in air, m^2/s
h_m	mass transfer coefficient, kg/m^2s
L	length of water panel, m
M	molecular weight
$\dot{m}_w$	rate of evaporation from the panel, kg/s
P	pressure, Pa
$P_{v\infty}$	partial pressure of water vapor outside the concentration boundary layer, Pa
DBT	dry bulb temperature, °C
WBT	wet bulb temperature, °C
T_w	water temperature in the panel, °C
u_∞	average free stream velocity in the wind tunnel, m/s
X_w	mole fraction of water vapor above the Interface.
X_w	mole fraction of water vapor in the free stream.
W	width of the wind tunnel, m

Greek Symbols

θ	wedge angle
δ	thickness of the wedges
β	area ratio parameter, $\delta/L.(\Delta A/A)$
μ	dynamic viscosity, $N.s/m^2$
ρ	density, kg/m^3
ΔP	pressure drop across the orifice, Pa
ϕ	relative humidity
ω	absolute humidity, $kg_{water}/kg_{dry\ air}$

Subscripts:

a	air
atm	atmospheric
B	bulk
e	exit
i	inlet
H_2O	water vapor
o	outlet
sat.	saturation
v	vapor
w	water, zero pressure gradient.
∞	free stream

Dimensionless groups:

Pr	Prandtle number, $Cp\ \mu/k$
Sc	Schmidt number , ν/D
Sh	Sherwood number, $h_m L/D$
Re	Reynolds number, $u_\infty L/\nu$

REFERENCES:

1. F. F. Araid, (1975),"Heat Transfer to Fluid Flow with Non-Uniform Velocity", M. Sc. Thesis, Mansoura University, Mansoura, Egypt.
2. G. Hesse, E. M. Sparrow and R. J. Goldstein, (1976), "Influence of Pressure on Film Boiling Heat Transfer", ASME Trans. J. of Heat transfer, Vol.5, pp.166-172.
3. A. C. Bajpai, I. M. Calus and J.A.Fairley, (1977), "Numerical Methods for Engineering and Scientests", John Wiely & Sons Ltd, New York.
4. F. P. Berger and K. F. Hau, (1979), "Local Mass Transfer Distribution on Surface Roughened with Small Square Ribs", Int. J. Heat Mass Transfer, Vol.22, pp.1645-1656.

5. S. J. Palaszewski, L. M. Jiji and S. A. Weinbaum, (1981), "Three Dimensional Air Vapour Droplet Interaction Model", ASME Trans. J. of Heat transfer, Vol.103, pp.514-521.
6. Chow, L. C. and Chung, J. N., (1983), "), "Evaporation of Water into Laminar Stream of Air and Superheated Steam", Int. J. Heat Mass Transfer, Vol. 26, No.3 , pp.373-380.
7. M. M. Awad, M. A. Shalaby and S. A. El-Shazly, (1986), "Compactness Effect of Air Plate Heat Exchangers of Convergent-Divergent Channels", Bulletin of the Faculty of Engincering, Mansoura University, Egypt, Vol.11, No.1.
8. J. C. Han, Y. M. Zhang and C. P. Lee, (1991), "Augmented Heat Transfer in a Square Channels with Parallel Crossed and V-Shaped Angled Ribs", Int. J. Heat Mass Transfer, ", Int. J. Heat Mass Transfer, Vol. 113, pp.590-596.
9. Sheikholeslami, R. and Watkinson, A. P., (1992), "Rate of Evaporation of Water into Superheated Steam and Humidified Air", Int. J. Heat Mass Transfer, Vol. 35, No.7 , pp.1743-1751.
10. G. S. Zheng and W. M. Worek, (1996), "Method of Heat and Mass Transfer Enhancement in Film Evaporation", Int. J. Heat Mass Transfer, Vol.39, No.1, pp.97-108.
11. Y. A. Cengel, (1998), "Heat Transfer: A Practical Approach", McGraw - Hill Company, New York.
12. S. S. Kachhwaha, P. L. Dhar and S. R. Kale, (1998), "Experimental Studies and Numerical Simulation of Evaporative Cooling of Air with a Water Spray. I- Horizontal Paralle Flow", Int. J. Heat Mass Transfer, Vol.41, No.2, pp.447-464.
13. S. S. Kachhwaha, P. L. Dhar and S. R. Kale, (1998), "Experimental Studies and Numerical Simulation of Evaporative Cooling of Air with a Water Spray. I- Horizontal Counter Flow", Int. J. Heat Mass Transfer, Vol.41, No.2, pp.465-474.
14. G. I. Sultan, A. M. Hamed and A. A. Sultan, (1999), "Effect of Inlet Parameters on the Performance of Packed Tower-Regenerator",
15. T. L. Cox and S. C. Yao, (1999), "Heat Transfer of Sprays of Large Water Drops Impacting on High Temperature Surface", ASME Trans. J. of Heat Transfer, Vol.121, pp.446-450.
16. Schwartze, J. P. and Brocker, S. (2000), "The Evaporation of Water into Air of Different Humidities and the Inversion Temperature Phenomenon", Int. J. Heat Mass Transfer, Vol. 43, No.6 , pp.1791-1800.
17. L. H. Rabie, A. A. Sultan and Y. E. Abdel Ghaffar, (2001), "Heat Transfer and Friction Loss in Periodically Converging-Diverging Variable Area Annuli", 12 th International Mechanical Power Engineering Conference (IMPEC-12), Mansoura, Egypt, October 30 Th-November 1 St, Vol.2, No. H13, pp. H167-H180.

Table (2) the dimensionless mass transfer coefficient ratio, Sh/Shw

Re		Convergent Configuration					Divergent Configuration				
	δ=0.0	δ=0.05	δ=0.075	δ=0.10	δ=0.125	δ=.137	δ=0.05	δ=0.075	δ=0.10	δ=0.125	δ=.1375
51660	1.00	1.101	1.357	2.278	2.025	1.093	1.0783	1.223	1.206	1.155	1.090
50780	1.00	1.047	1.235	2.083	1.356	1.052	0.9391	1.091	1.167	1.094	1.025
46990	1.00	1.026	1.375	1.850	1.454	1.179	1.0438	1.151	1.336	1.172	1.198
38070	1.00	1.125	1.380	2.074	1.549	1.153	0.8086	1.115	1.430	1.118	1.137
28760	1.00	1.211	1.574	1.927	1.704	1.055	0.9091	1.026	1.563	1.103	1.041
22630	1.00	1.069	1.523	2.006	1.704	1.151	0.9457	0.913	1.751	0.729	1.035
11000	1.00	1.621	1.538	2.971	1.875	1.287	1.0735	1.380	2.135	0.717	0.990

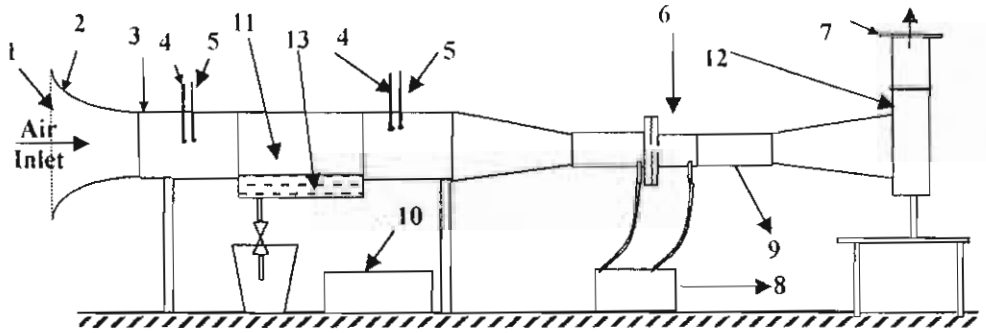

Fig.(1) Schematic diagram of the experimental apparatus.

1. mesh screen, 2. Bell-mouth inlet, 3. Wind tunnel, 4. Wet bulb thermometer, 5. Dry bulb thermometer, 6. Orifice meter, 7. Flow rate gate, 8. Micro-manometer, 9.Flexible connection, 10. Mass balance. 11.Test section, 12. Blower, 13. Water panel, 14. Wooden wedges. 15. pressure tapes

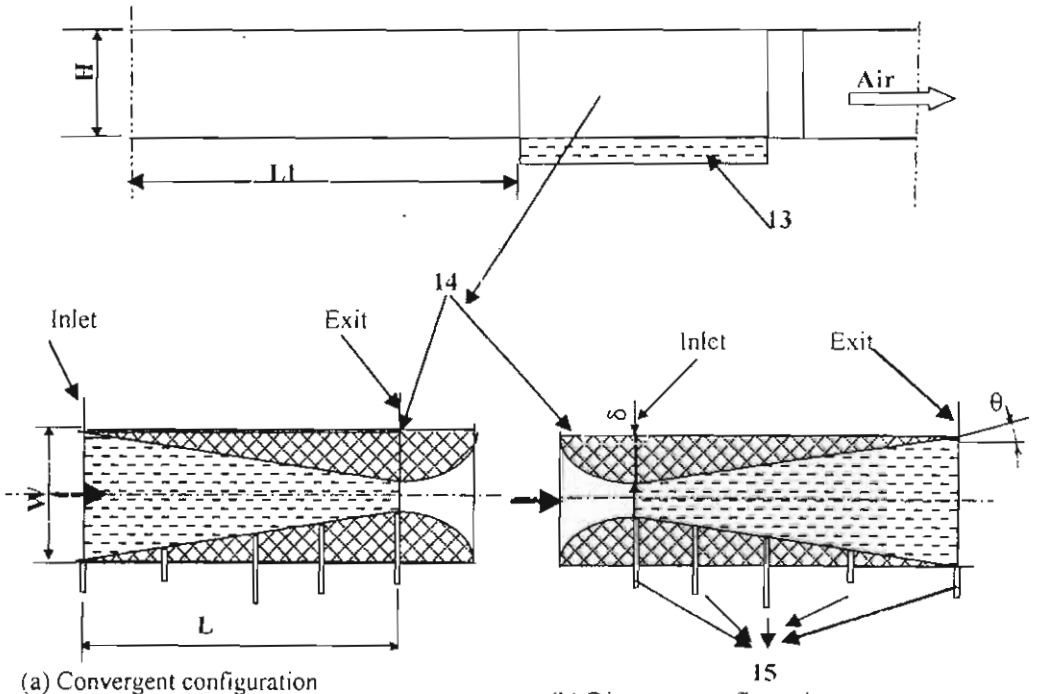

(a) Convergent configuration

(b) Divergent configuration

Fig (2) Details of Test Rig

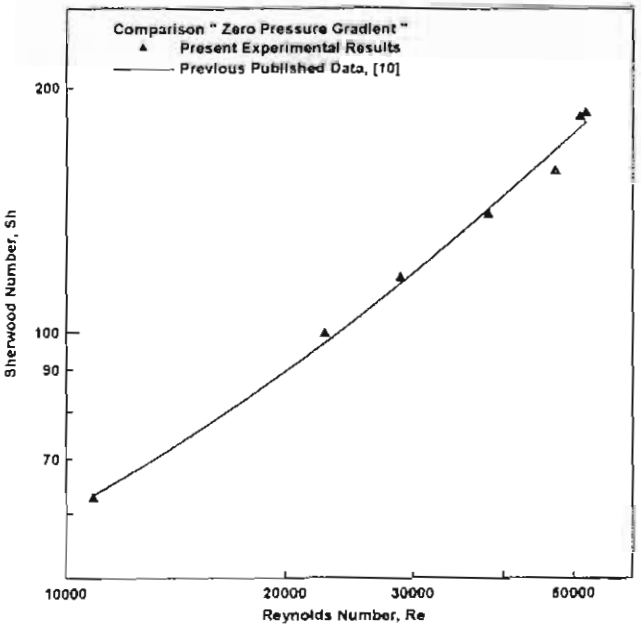

Fig. 3 Comparison of the present experimental data with the data of Zheng et al., [10].

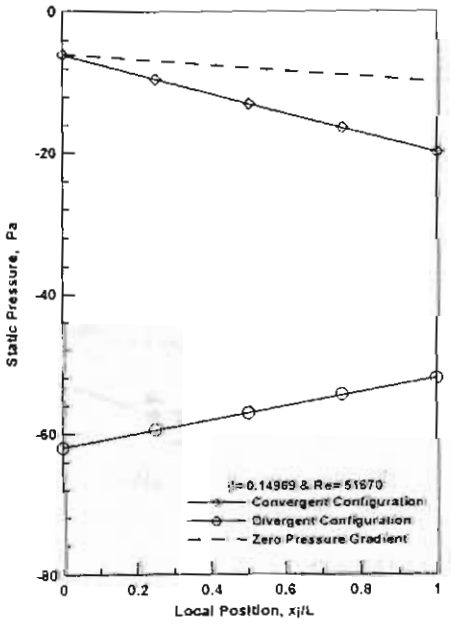

Fig. 4 Static pressure along the test section for both positive and negative pressure gradient configurations at constant area ratio parameter and Reynolds number.

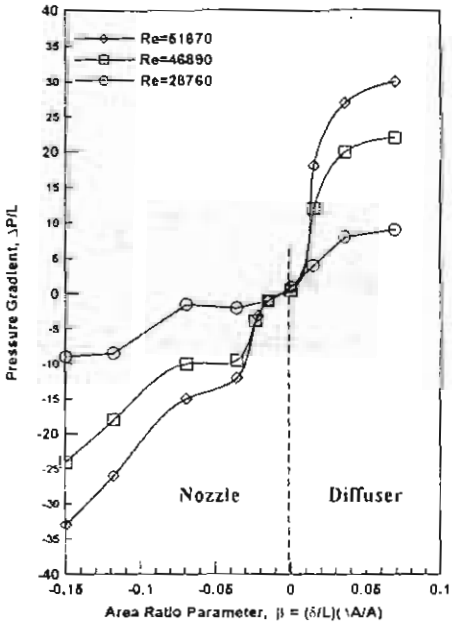

Fig. 5 Pressure gradient versus area ratio at different values of Reynolds number for negative and positive pressure gradient configurations.

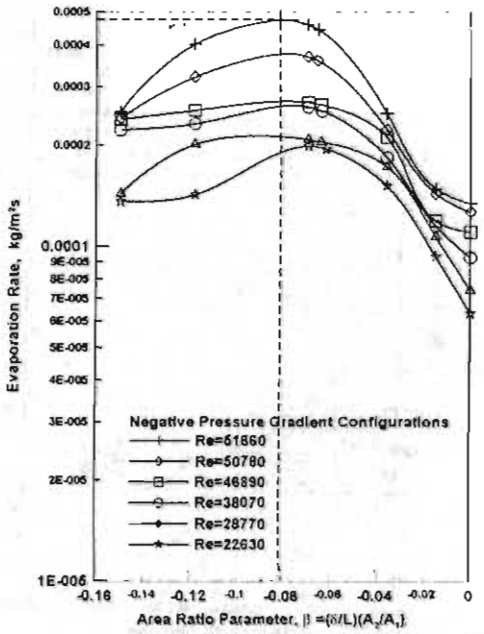

Fig. 6 Evaporation rate versus area ratio parameter at different values of Reynolds number for negative pressure gradient configurations.

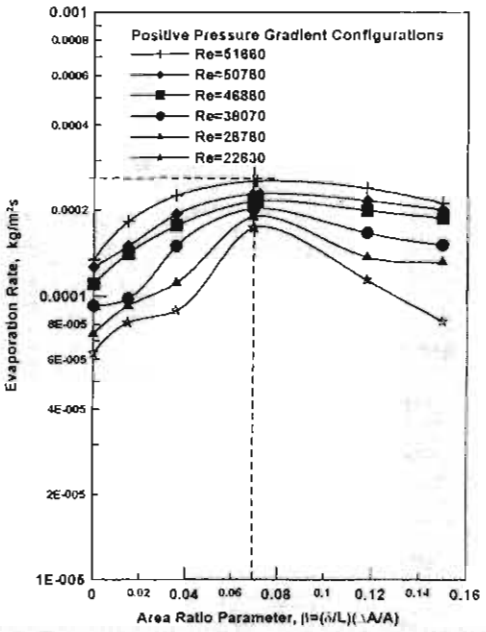

Fig. 7 Evaporation rate versus area ratio parameter at different values of Reynolds number for positive pressure gradient configurations.

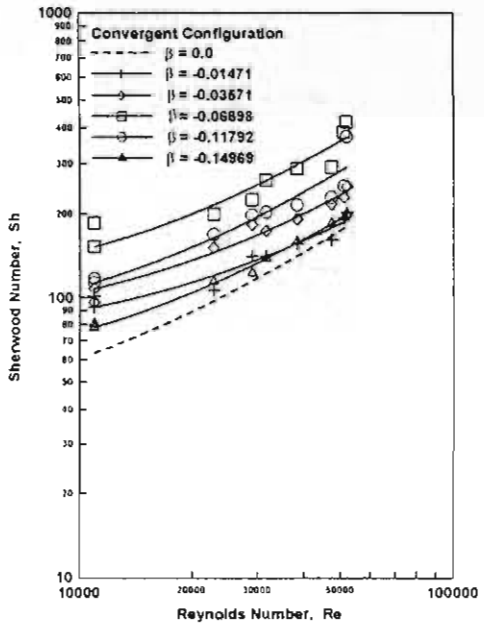

Fig. 8 Sherwood number versus Reynolds number at different values of area ratio parameter factors for convergent configuration.

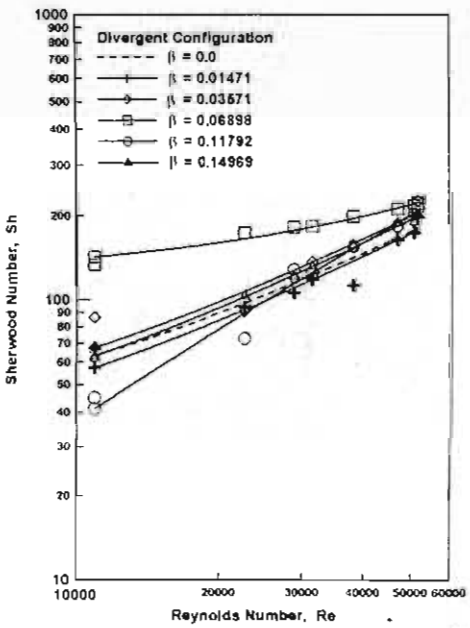

Fig. 9 Sherwood number versus Reynolds number at different values of area ratio parameter for divergent configuration.

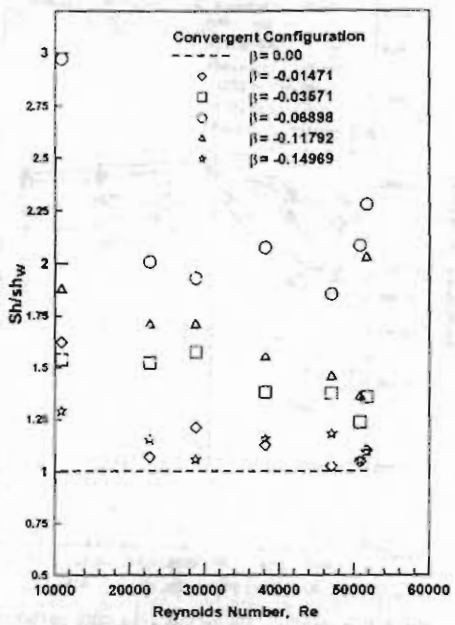

Fig. 10 The mass transfer coefficient ratio versus Reynolds number at different values of area ratio parameter for convergent configurations.

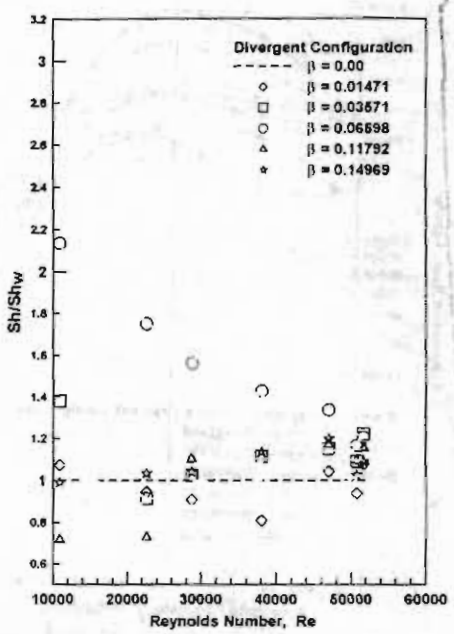

Fig. 11 The mass transfer coefficient ratio versus Reynolds number at different values of area ratio parameter for divergent configurations.

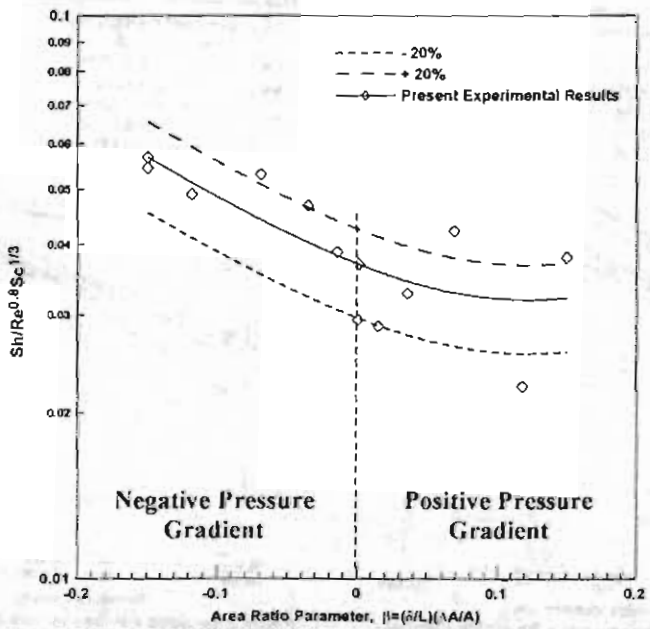

Fig. 12 Correlation of the present experimental result for both positive and negative pressure gradient configurations.